

# Room temperature continuous wave milliwatt terahertz source

Maik Scheller<sup>1,2</sup>, Joe M. Yarborough<sup>1,3</sup>, Jerome V. Moloney<sup>1,3</sup>, Mahmoud Fallahi<sup>1,3</sup>,  
Martin Koch<sup>1,2</sup>, and Stephan W. Koch<sup>1,2</sup>

<sup>1</sup>Desert Beam Technologies LLC, 3542 N Geronimo Avenue, Tucson, AZ 85705, USA

<sup>2</sup>Fachbereich Physik, Philipps-Universität Marburg, Renthof 5, 35037 Marburg, Germany

<sup>3</sup>College of Optical Sciences, University of Arizona, 1630 E University Boulevard, Tucson, AZ, 85721, USA

\*maik.scheller@physik.uni-marburg.de

**Abstract:** We present a continuous wave terahertz source based on intracavity difference frequency generation within a dual color vertical external cavity surface emitting laser. Using a nonlinear crystal with a surface emitting phase matching scheme allows for high conversion efficiencies. Due to the tunability of the dual mode spacing, the entire spectral range of the terahertz gap can be covered. The terahertz output scales quadratically with the intracavity intensity, potentially allowing for terahertz intensities in the range of 10s of milliwatts and beyond.

©2010 Optical Society of America

**OCIS codes:** (300.6495) Spectroscopy, terahertz; (250.5960) Semiconductor lasers.

---

## References and links

1. D. Grischkowsky, S. Keiding, M. Exter, and C. Fattinger, "Far-infrared time-domain spectroscopy with terahertz beams of dielectrics and semiconductors," *J. Opt. Soc. Am. B* **7**(10), 2006–2015 (1990).
2. C. Debus, and P. H. Bolivar, "Frequency selective surfaces for high sensitivity terahertz sensing," *Appl. Phys. Lett.* **91**(18), 184102 (2007).
3. T. Yasui, T. Yasuda, K. Sawanaka, and T. Araki, "Terahertz paintmeter for noncontact monitoring of thickness and drying progress in paint film," *Appl. Opt.* **44**(32), 6849–6856 (2005).
4. C. D. Stoik, M. J. Bohn, and J. L. Blackshire, "Nondestructive evaluation of aircraft composites using transmissive terahertz time domain spectroscopy," *Opt. Express* **16**(21), 17039–17051 (2008).
5. C. Jördens, and M. Koch, "Detection of foreign bodies in chocolate with pulsed terahertz spectroscopy," *Opt. Eng.* **47**(3), 037003 (2008).
6. A. J. Fitzgerald, B. E. Cole, and P. F. Taday, "Nondestructive analysis of tablet coating thicknesses using terahertz pulsed imaging," *J. Pharm. Sci.* **94**(1), 177–183 (2005).
7. P. H. Siegel, "Terahertz technology in biology and medicine," *IEEE Trans. Microw. Theory Tech.* **52**(10), 2438–2447 (2004).
8. P. H. Siegel, "THz Instruments for Space," *IEEE Trans. Antenn. Propag.* **55**(11), 2957–2965 (2007).
9. B. S. Williams, "Terahertz quantum-cascade lasers," *Nat. Photonics* **1**(9), 517–525 (2007).
10. C. Walther, M. Fischer, G. Scalari, R. Terazzi, N. Hoyler, and J. Faist, "Quantum cascade lasers operating from 1.2 to 1.6 THz," *Appl. Phys. Lett.* **91**(13), 131122 (2007).
11. M. I. Amanti, M. Fischer, G. Scalari, M. Beck, and J. Faist, "Low-divergence single-mode terahertz quantum cascade laser," *Nat. Photonics* **3**(10), 586–590 (2009).
12. E. Rouvalis, C. C. Renaud, D. G. Moodie, M. J. Robertson, and A. J. Seeds, "Traveling-wave Uni-Traveling Carrier photodiodes for continuous wave THz generation," *Opt. Express* **18**(11), 11105–11110 (2010).
13. S. Hayashi, T. Shibuya, H. Sakai, T. Taira, C. Otani, Y. Ogawa, and K. Kawase, "Tunability enhancement of a terahertz-wave parametric generator pumped by a microchip Nd:YAG laser," *Appl. Opt.* **48**(15), 2899–2902 (2009).
14. W. C. Hurlbut, V. G. Kozlov, and K. L. Vodopyanov, "Difference frequency generation of THz waves inside a high-finesse ring-cavity OPO pumped by a fiber laser," *Conference on Lasers and Electro-Optics (CLEO) and Quantum Electronics and Laser Science Conference (QELS)*, 2010.
15. R. Sowade, I. Breunig, I. Cámara Mayorga, J. Kiessling, C. Tulea, V. Dierolf, and K. Buse, "Continuous-wave optical parametric terahertz source," *Opt. Express* **17**(25), 22303–22310 (2009).
16. L. Fan, M. Fallahi, J. Hader, A. R. Zakharian, J. V. Moloney, W. Stolz, S. W. Koch, R. Bedford, and J. T. Murray, "Linearly polarized dual-wavelength vertical-external-cavity surface-emitting laser," *Appl. Phys. Lett.* **90**(18), 181124 (2007).
17. J. V. Moloney, J. Hader, and S. W. Koch, "Quantum design of semiconductor active materials: laser and amplifier applications," *Laser Photon. Rev.* **1**(1), 24–43 (2007).
18. J. A. Lhuillier, G. Torosyan, M. Theuer, Y. Avetisyan, and R. Beigang, "Generation of THz radiation using bulk, periodically and aperiodically poled lithium niobate. Pt.1: Theory," *Appl. Phys. B* **86**(2), 185–196 (2007).

## 1. Introduction

Continuous wave (CW) terahertz (THz) sources are highly desirable for a wide range of applications ranging from spectroscopy [1] and biosensing [2] over quality inspection in various industrial branches [3–5], to medical and pharmaceutical applications [6,7]. Another potential application field is the THz astronomy [8], where high power sources are required to drive heterodyne receivers at key frequencies (e.g. 1.4, 1.9, 2.7 THz). Particularly in the frequency range between 1 and 5 THz it is still challenging to generate decent power levels with tunable room temperature devices.

While the development of quantum cascade lasers (QCLs) is progressing and the beam shape and output powers of these devices are steadily improving [9–11], QCLs still require cryogenic cooling. As an alternative, THz emitters based on photomixing in semiconductor photoconductive antennas or THz photodiodes [12] are discussed. However, in this case the finite carrier lifetime of semiconductor materials induces a pronounced roll-off at higher frequencies that scales down the available THz power beyond 1 THz to few  $\mu$ Ws.

Another promising approach is the parametric frequency conversion of infrared laser light into THz waves. The generation of several  $\mu$ W's of narrow band pulsed THz radiation has been shown recently using Q-switched pump lasers [13,14]. Yet, to generate pure CW THz radiation, CW pump lasers are required. Since the parametric conversion efficiency scales quadratically with the infrared peak intensity, lower THz powers will result. Up to now even sophisticated optical parametric oscillator schemes deliver only CW THz powers below 3  $\mu$ W [15].

Here, we present a compact, tunable room temperature operating CW source capable of generating THz radiation with milliwatt power levels at frequencies of 1 and 1.9 THz. The system is based on intracavity difference frequency generation (DFG) within a dual color vertical external cavity surface emitting laser (VECSEL). Utilizing the extremely high circulating intracavity fields to mix the two modes within a nonlinear crystal results in an efficient generation of THz waves. The direct conversion within the laser cavity does not only provide the access to the highest infrared intensities but allows for a relatively simple and robust setup at the same time.

In previous work, it was demonstrated that a VECSEL can emit dual wavelength simultaneously using an intracavity filter to select the desired laser modes [16]. The high bandwidth of the quantum wells used as gain region of tens of nm [17] is favorably for the generation of a wide range of THz frequencies. To achieve the mW results reported here, we utilized a cavity design that includes an intracavity nonlinear crystal. This intracavity DFG generation scheme is not only capable of reaching power levels of several mW but also has the advantage of accessing THz frequencies beneath and well above 1 THz since the parametric mixing process has no roll-off frequencies known from the finite carrier lifetime of semiconductor materials.

## 2. Experimental setup

The heart of our new THz source is a VECSEL chip with an emission wavelength around 1030 nm that is mounted on a water cooled heat sink and is pumped by an external, fiber coupled semiconductor laser bar emitting around 808 nm. The maximum used pump power was 50 W. At this maximal pump levels the pump laser consumes less than 250 W of electric power. The free-running VECSEL will normally emit many laser wavelengths. However, by inserting an etalon into the cavity, we force the laser to run simultaneously on two wavelengths with a predefined frequency spacing.

A schematic plot of the VECSEL cavity is shown in Fig. 1 (left) and a photograph of our experimental setup is presented on the right hand side of the figure. The cavity consists of the VECSEL chip, a curved mirror and a plane mirror, an etalon made of quartz, a Brewster window and the nonlinear crystal. Both mirrors are highly reflecting. This configuration is the

simplest to realize dual- or multi-wavelength operation of the device. The footprint of this arrangement is relatively compact (approx. 20 cm x 20 cm) and can be further reduced in size. However, the pump laser (dimensions of 33 cm x 17 cm x 7 cm) is also part of the setup. Example spectra of the observed dual wavelength VECSEL operation are shown in Fig. 2. As can be seen in the figure, a slight tilting of the etalon allows for tuning of the difference frequency and thus, to vary the frequency of the generated THz wave. However, the tuning range of this technique is limited to about 200 GHz. If higher ranges are required, one could either use a set of different thick etalons or an air spaced etalon with variable thickness. As representative examples, we focus here on the generation of 1 THz and 1.9 THz, respectively. For this study, we used two differently thick etalons and two differently poled crystals to achieve optimal generation efficiencies. Specifically, the etalons consist of uncoated quartz with a thickness of 100  $\mu\text{m}$  and 54  $\mu\text{m}$  for 1 THz and 1.9 THz, respectively. The slanting angle of the crystal poling is  $67^\circ$  and the poling periods are 58  $\mu\text{m}$  for 1 THz and 29  $\mu\text{m}$  for 1.9 THz.

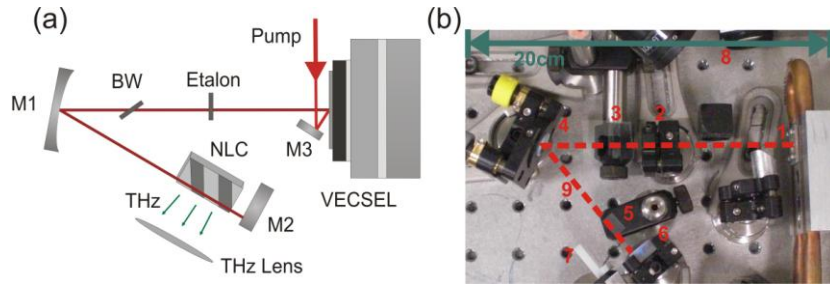


Fig. 1. (a): Illustration of the setup: The pump laser is reflected by the mirror M3 and directed to the VECSEL chip. The cavity is formed by the curved mirror M1 and the flat mirror M2. A Brewster window (BW) and an etalon are placed within the resonator to ensure a linear polarized emission at two wavelengths. The two laser modes mix inside the nonlinear crystal (NLC) and THz radiation is emitted from the crystal surface, collimated by a cylindrical THz lens. (b): Photograph of the employed setup. The marked parts are 1) the semiconductor VECSEL device, 2) the etalon, 3) the BW 4) M1, 5) the NLC, 6) M2, 7) a cylindrical THz lens, 8) the head of the pump laser and 9) the illustrated circulating IR laser mode.

The employed nonlinear element is a 5% MgO-doped congruent lithium niobate crystal that is 10 mm long, 5 mm wide and 1 mm thick. The crystal exhibits a slanted periodical poling [18] that is designed for an efficient conversion around a center frequency. The phase matching bandwidth is about 250 GHz. This special kind of crystals exhibit a surface emitting phase matching scheme, so that the THz waves are intrinsically separated from the laser radiation.

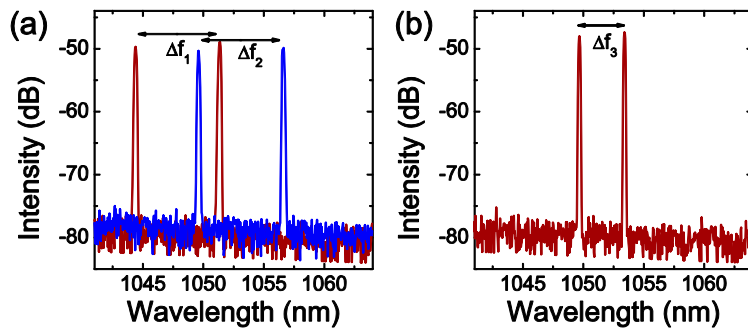


Fig. 2. (a): Recorded spectrum at dual (2-color) wavelength emission of the VECSEL for two tilt angles of a 40  $\mu\text{m}$  thick silica etalon  $\Delta f_1 = 1.90$  THz,  $\Delta f_2 = 1.85$  THz. (b) Spectrum with a different etalon that causes a difference frequency of  $\Delta f_3 = 1$  THz.

Due to the asymmetric geometry of the THz generation region (the length of the crystal is 10 mm and the laser modes diameter is about 200  $\mu\text{m}$ ), the emitted THz beam is expected to

be collimated in one axis and divergent in the other. To correct this, we used a cylindrical polyethylene lens to collimate the divergent axis of the beam. A second spherical lens (not shown) is used to focus it onto a Golay cell. To increase the collection efficiency, we utilized a tapered metal tubule placed directly in front of the detector aperture. The Golay cell was fabricated by Microtech Instruments and has a responsivity in the order of  $10^4$  V/W. The calibration details were supported by the manufacturer. To attenuate the THz signal below the saturation limit of the Golay cell we used up to 10 sheets of black polyethylene that we characterized in terms of their transmittance. These sheets also serve as blocking filters for the infrared light, so that the power measurement is not disturbed by a leakage of infrared power into the Golay cell.

### 3. Measurements

We placed the nonlinear crystal close to the highly reflecting flat mirror (M2 in Fig. 1) because at this point the laser mode reaches its minimum beam waist of around  $100\text{ }\mu\text{m}$ . The two highly intense infrared laser modes induce a nonlinear polarization in the crystal that oscillates with the difference frequency. This polarization is the source of the emitted THz wave. The THz radiation is coupled out of the crystal facets perpendicular to the propagation direction of the laser beam. Figure 3 shows the measured THz power together with a quadratic fit of THz versus intracavity power that agrees very well with the data. This quadratic scaling is expected for a DFG process [19]. The THz signal at 1.9 THz exceeds 2 mW at intracavity power levels of 500 W. At 1 THz, the measured power reached 0.5 mW supporting the additional theoretical expectation that the conversion efficiency of the employed phase matching technique should improve with increasing frequencies. Since the reflectivity of the high reflective mirrors is known, the infrared intracavity power was determined by measuring the transmitted power through one of the laser mirrors.

While the THz radiation is emitted in two directions perpendicular to the infrared laser modes, we only measured the THz waves coupled out from one of the crystal facets. The crystal surface was also not anti-reflective coated for the THz wavelength so that the reflection losses exceed 40%. Consequently, the measured THz signal shown in Fig. 3 is below the total generated THz power within the crystal.

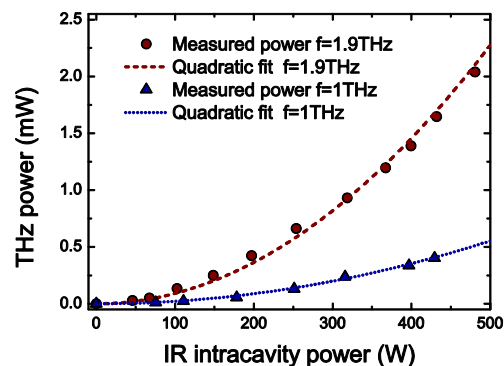


Fig. 3. (a): Measured THz output power as function of the total intracavity power of both infrared modes. The THz frequency was 1 THz (triangles) and 1.9 THz (dots). The quadratic fit functions represent the expected behavior of the intracavity difference-frequency generation scheme [19].

To measure the frequency of the generated THz waves, we set up a Michelson interferometer consisting of a polymeric beam splitter and two gold mirrors. One of the mirrors was mounted on a translation stage. Figure 4 shows the signal detected by the Golay cell as a function of the mirror position together with a fit for 1.9 THz. As expected from

energy conversion, the measured THz frequency agrees with the difference frequency between the two laser modes, measured with an optical spectrum analyzer.

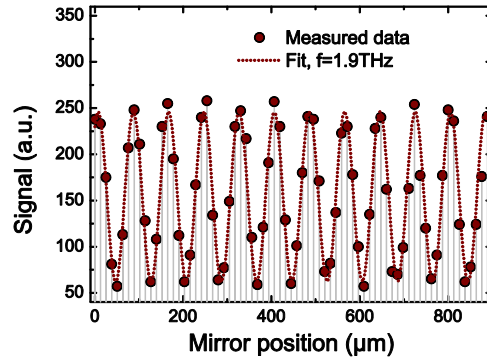


Fig. 4. Signal of the Michelson interferometer setup as function of the mirror position together with a fit for 1.9 THz.

The beam shape was characterized by translating the Golay cell in x and y direction at a distance of 30 cm from the cylindrical collimation lens. To increase the spatial resolution, we placed a 3 mm diameter aperture in front of the detector. The intensity profile shown in Fig. 5 has an almost perfect Gaussian shape. Similar results are obtained from measurements with different spacing between the detector and the lens indicating a preferable beam profile of the emitted radiation.

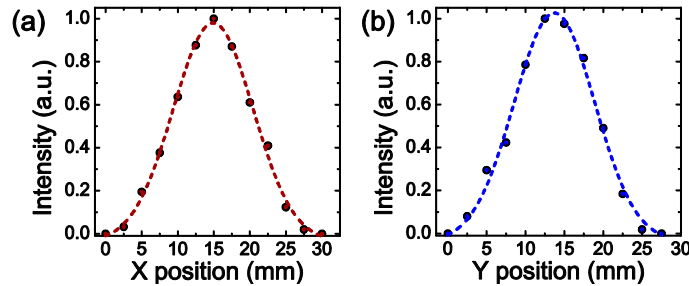


Fig. 5. Beam shape of the collimated THz radiation measured through a 3 mm aperture before the Golay cell. Measured values for a scan along the x (a) and y (b) axis together with a Gaussian fit.

#### 4. Conclusion

The experiments presented here demonstrate the potential of our new CW THz source which makes use of the extremely high circulating intracavity fields in the VECSEL. In these experiments the laser was free running. Future efforts will concentrate on frequency stabilization to minimize the linewidth of the generated THz radiation. In the presented setup the frequency tunability is restricted by the employed etalon and the nonlinear crystal. Using other wavelength filter elements and crystals with broadband phase matching bandwidths like aperiodically poled lithium niobate or emitters for Cherenkov radiation [18] will allow for free tunability within the THz wavelength regime. At the present state the heat sink was based on water cooling. The use of compact, thermo electric cooling is part of the ongoing work. Besides, the basic configuration allows for a clear power scalable strategy by using either higher pump powers or cavity optics with lower losses to increase the fundamental intracavity intensity.

### **Acknowledgements**

We acknowledge stimulating discussions with C. Walker, C. d'Aubigny, and A. Young, Steward Observatory and Dept. of Astronomy, University of Arizona. We furthermore thank HC Photonics Corp, Taiwan for manufacturing our custom designed nonlinear crystals.